VOLTAGE SOURCE CONVERTOR TOPOLOGY FOR HVDC GRID CONNECTION OF OFFSHORE WINDFARMS

Shivani Kumari[1], Jyotsana[2]
UG, [1,2] Department of Electrical and Electronics Engineering,
Raj Kumar Goel institute of technology for Women, UP (India)

ABSTRACT

Large offshore wind farms are recently emerging as promising alternative power Sources. Long distances between offshore generation and onshore distribution grid demand new solutions for their connect alternative to conventional AC transmission above a certain cable length. This paper presents a new VSC transmission topology for HVDC grid connection of offshore wind farms.

Keywords: RE Power sytem, VSC transmission, IGBT.

I INTRODUCTION

The recent emergence of larger and more efficient wind turbines establishes bright prospects in wind power generation. The first 5 MW wind turbine was erected in Brunsbüttel near Hamburg in summer 2004 by RE power Systems AG. These latest developments extend the potential of large-scale offshore wind generation, which becomes a rapidly growing worldwide alternative power source.

Today, especially large offshore wind farms in the power range of several hundred megawatts are getting into focus. Limited availability of onshore sites and better offshore wind conditions are driving the wind turbines offshore. Environmental requirements regarding noise pollution and the visible impact as well as colliding interests in the near shore areas (recreation, military, coastal shipping, fishing etc.) lead to increasing distances between offshore wind farms and onshore distribution grids. Remote locations, however, often imply deep water depths, complicating the foundation of the wind turbines in the seabed. Recent improvements in submarine foundations (i.e. tripod, quadropod or lattice structures) allow deeper water depths, whereas the current economic limit of such installations lies in the range of 30 to 35 m. Another important factor that causes prolonged transmission distances is the necessity of a strong grid connection point with a significant short-circuits capacity. Reaching a suitable AC network connection point requires often a long onshore transmission line. In exchange, expensive grid enforcement measures can be avoided. As a consequence of the ongoing trend, the generated power from the wind farms has to be transported over longer distances in order to make a connection to the AC network for onward transmission and distribution. For longer transmission distances, HVDC transmission is a feasible solution compared to traditional AC transmission. AC cables inherently generate reactive power that limits the maximum permissible AC cable length. This is known as the critical AC cable length.

The critical cable length for AC transmission cannot be determined generally. It varies for every individual project and is given by economical and technical constraints. Nowadays, it lies in the range of approximately 100 km. As mentioned before, the AC cable length is limited due to capacitive charging currents. Above a certain cable length, a compensation unit is required. This is particularly costly and troublesome for submarine cables.

HVDC transmission systems based on VSCs, also called VSC transmission, have lately emerged as a competitive alternative to conventional AC transmission. Their operation principle is shown in Fig. 1. VSC transmission provides an efficient and reliable solution overcoming the major technical difficulties facing traditional AC solutions. Mainly, DC cables are not affected by cable charging currents and thus can have any length required. The DC cable capacitance offers instead the advantage of energy storage. Only the cost of the complex onshore andoffshore converter stations and the losses of the semiconductor devices limit an augmented application of VSC transmission. Especially the high frequency PWM switching leads to excessive switching losses. Thus, an improvement in efficiency and lower initial converter costs are highly attractive and help to decrease the minimum length at which VSC transmission can compete with traditional AC transmission

VSC transmission offers a couple of additional advantages compared to AC transmission. If there are environmental constraints on the quantity of submarine cables, DC cables with a higher capacity are the preferable choice. Furthermore, VSC transmission allows frequency control of the local wind farm grid, as the frequencies on both ends of the DC link are independent. Both the active power flow and reactive power at both ends of the DC link are fully defined and controllable. This allows the control of voltage fluctuations and increases the exchange limits of reactive power, thus stabilizing the AC grid at the connection point. The electrical impact of the VSC transmission on the existing AC network, as i.e. the harmonic distortion must be studied.

In this paper, a new soft-switched VSC topology is proposed that promises both lower initial costs and a higher efficiency. As a consequence, the minimum cable length at which VSC transmission gets interesting can be further decreased and the HVDC grid connection of large offshore wind farms gets far more attractive. The operation principle of this new VSC topology is presented with respect to the commutation of the semiconductor switches. The advantages and challenges of the proposed topology are also outlined. Furthermore, a comparison with a state-of-the-art variable-speed wind turbine reveals the potential of this new technology. Thereby, this paper concentrates on the losses and ratings of the converters.

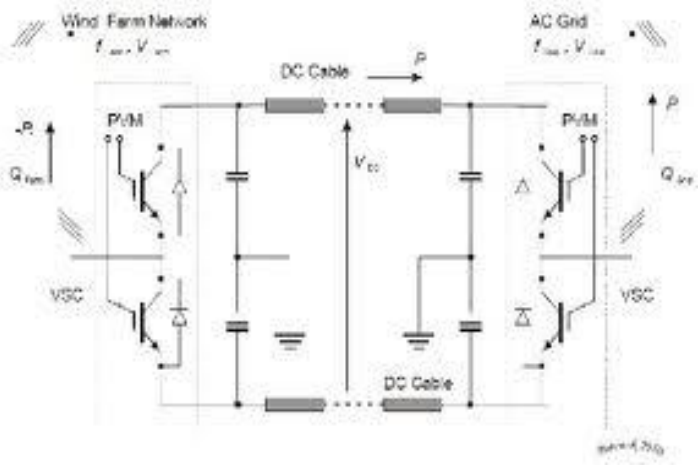

Fig. 1. Principle of VSC transmission

II DESCRIPTION OF PROPOSED TOPOLOGY

The topology of the proposed AC/DC converter is shown in Fig. 2. It incorporates a VSC and cycloconverters (direct converters) connected via a medium frequency (MF)

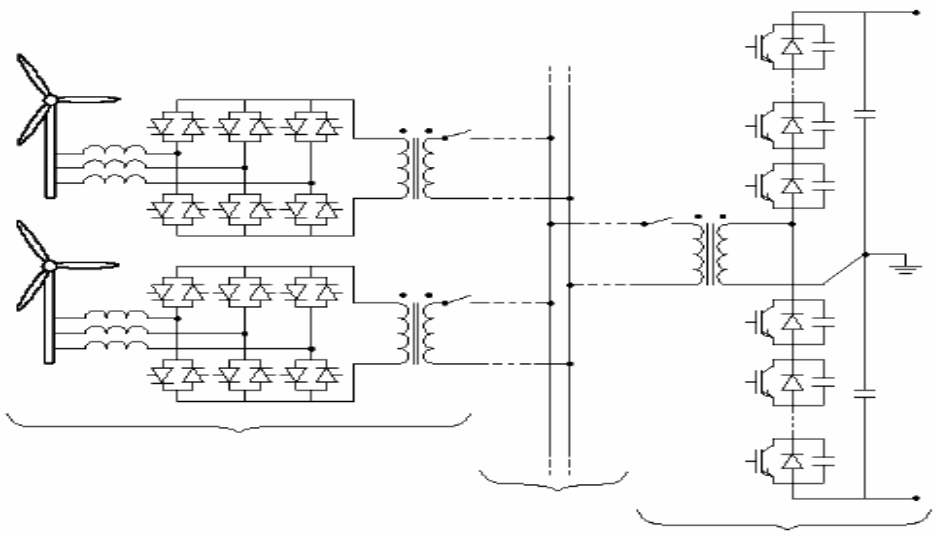

Fig. 2. The Schematic Of Proposed Technology

Every wind turbine is equipped with a passive line filter, a 3-by-2 cycloconverter, an MF transformer and a circuit breaker. This enables the individual wind turbine to operate as an adjustable-speed generator (ASG), offering multiple advantages compared to fixed-speed operation, as i.e. increased efficiency. The valves of the cycloconverter do not need any turn-off capability and can be realized by fast thyristors connected in anti-parallel. The MF transformer increases the generator voltage from 690 V to 33 kV. The high-voltage side of the transformer is connected to the MF AC bus via a circuit breaker allowing the disconnection of the wind turbine.

This MF AC bus connects the wind turbines to a single-phase VSC via the main circuit breaker and the main MF transformer. This transformer increases the bus voltage from 33 kV to half the DC link voltage (150 kV). The high-voltage side of the transformer is connected to a single-phase VSC, whereas one of the transformer terminals is connected to the midpoint in the DC link created by bus-splitting capacitors. These DC capacitors provide the DC voltage source necessary for the dynamics of the system and govern the voltage ripple on the DC line. Series-connected IGBTs with ant parallel diodes form the valves of the VSC. Additionally, the VSC is equipped with snubber capacitors connected in parallel to each of the semiconductor switches. The capacitors should be sufficiently large to allow zero-voltage turn-off of the IGBTs. The ground reference of the VSC is made at the midpoint in the DC link.

2.1 Principle of Operation

By alternately commutating the cycloconverters and the VSC it is possible to achieve soft commutations for all the semiconductor valves. The cycloconverter can be solely operated by line commutation (natural commutation) whereas snubbered or zero-voltage commutation is always enabled for the VSC. The operation principle during a commutation sequence is described below. The VSC is commutated at fixed time instants with constant intervals (switching frequency *mf* = 500 Hz), thus generating an MF square-wave voltage on the AC bus. When the main transformer current and voltage have the same sign (instantaneous power flow is directed from the DC-side to the AC-side), the conditions are set for a snubbered commutation of the VSC. The process is initiated by turning off the conducting valve at zero-voltage conditions. The current is thereby diverted to the snubber capacitors. The antiparallel diodes of the incoming valve take over the current once the potential of the phase terminal has fully swung to the opposite. At this stage, the IGBTs that are antiparallel to the diodes can be gated on at zero-voltage zero-current conditions. Reversing the transformer voltage during the VSC commutation establishes the possibility for natural commutation of the cycloconverters. The commutation of a cycloconverter phase leg is initiated by turning on the nonconducting valve in the direction of the respective phase current. The VSC voltage and the leakage inductances of the transformers govern the natural commutation. Finally, the initially conducting thyristor turns off as the current through it goes to zero. The cycloconverter phase legs are commutated in order to obtain the desired PWM generator voltages. Additionally, successive commutations of the cycloconverter phase legs eventually lead to a reversal of the current through the main MF transformer, thus setting the conditions for a snubbered commutation of the VSC.

2.2 Advantages And Challenges

The proposed AC/DC converter topology offers multiple advantages in addition to the basic features of conventional VSC transmission systems. In order to ensure proper functioning of the topology, however, certain technical challenges have to be analyzed.

Lower initial costs are a main ambition of the new proposed topology. Among other things, this is achieved by utilizing cheaper single-phase MF transformers. A positive side-effect is the reduction in weight and volume that simplifies their integration in the wind turbines. The design of the MF transformers has to be adapted to the specific characteristics of the proposed topology. Especially the design of the transformer insulation needs to withstand high voltage derivatives (however limited by the VSC snubber capacitors). Another factor that decreases the initial costs is the significant reduction in the number of series-connected IGBT valves in the VSC. A reduction is highly desirable, as IGBTs tend to be expensive and require complex gate drives and voltage-sharing circuitries. SECTION VI presents the possible savings. On the other hand, the cycloconverters entail additional costs, even though their valves consist of comparably cheap and well-established fast thyristors.

An increase of the converter efficiency is crucial, especially during low power generation. Otherwise, the converter losses may consume a significant portion of the generated power. The switching losses are reduced considerably (refer to SECTION VI) by using a soft-switching commutation scheme. Moreover, the thyristors in the cycloconverters have low losses compared to IGBTs. An important factor determining the system efficiency is the influence of the non-sinusoidal square-wave MF AC voltage on the losses in the AC cables. Finally, the design of the control system has to be optimized in terms of ensuring maximum overall efficiency.

III DESCRIPTION OF REFERENCE TOPOLOGY

Today, the predominant solution for adjustable-speed wind turbines is the doubly-fed induction generator (DFIG) ASG. Its configuration is shown in the lower part of Fig. 3. The stator of the induction generator is directly connected to the wind farm grid whereas the rotor windings are connected to a frequency converter (back-to-back VSC) over slip rings. This allows the wind turbine to operate over a wide speed range, depending on the rating of the back-to-back VSC. Unlike the new proposed topology, however, the solution with a DFIG requires slip rings (costly and maintenance intensive in an offshore environment) and does not enable full adjustable-speed operation. Nevertheless, DFIG is currently the preferable solution when the wind turbines are directly connected to the main AC grid.

To ensure comparability, the reference topology should feature the same characteristics as the proposed topology. Thus, this paper focuses on a comparison with the direct-inline ASG. Its configuration is shown in the upper part of Fig. 3. Every wind turbine generator is connected to the wind park grid over a full-size frequency converter. This back-to-back VSC requires the same rating as the wind turbine generator and is therefore very expensive. In return, a simple squirrel cage induction generator can be applied. This topology offers all advantages of adjustable speed operation.

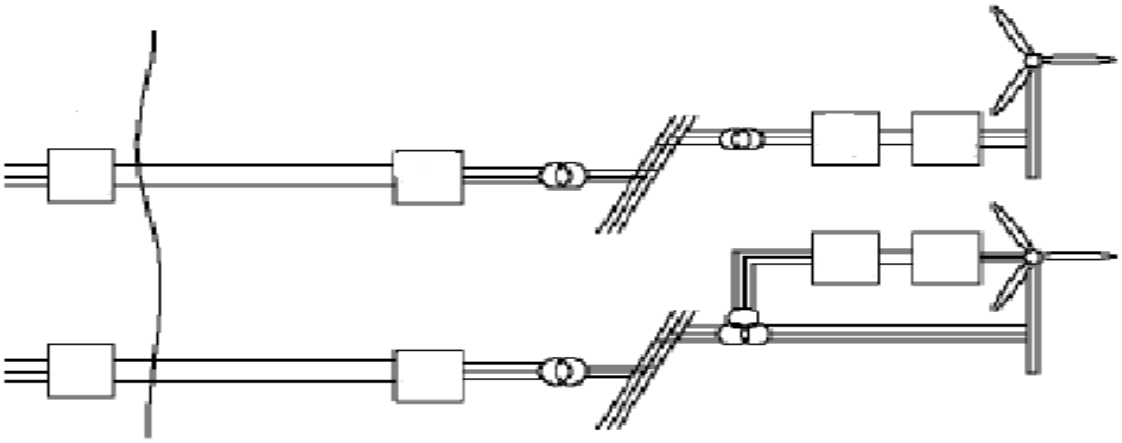

Fig 3. Reference topology. (1)Direct-In-Line ASG, (2) Doubly-fed Induction generator

The onshore three-phase VSC linking the AC network to the submarine DC cable is not considered in this comparison, as it is independent of the offshore converters. On the other side, different topologies are suitable for the offshore three-phase VSC, e.g. two-level, multilevel diode-clamped or multilevel floating capacitor converters. In this comparison, the topology applied is assumed to be a hard-switched two-level converter, which is an established solution in VSC transmission systems. The frequency modulation ratio (PWM switching frequency divided by fundamental frequency) is p = 39 and the fundamental frequency is $f0$ = 50 Hz. It is assumed that the amplitude modulation ratio for the hard switched reference topology is increased to ma = 1.1 by third harmonic injection. On the other hand, the amplitude modulation ratio for the proposed soft-switching topology is chosen as ma = 0.9 to provide the possibility of increasing the voltage if necessary.

IV IGBT LOSSES AND RATINGS

This section presents the procedures applied to determine the IGBT conduction and switching losses of the different VSCs, namely the single-phase VSC in the proposed soft-switched topology and the three-phase VSC as well as the back-to-back VSCs in the hard-switched reference topology. The IGBT losses are an essential factor regarding the thermal design and influence the current rating of the IGBT. This current rating along with the voltage rating of the IGBT determines the power rating, which is an important indicator of the costs for the IGBTs. Generally, the converter rating should be increased by a certain margin that offers the possibility for i.e. regenerative braking. In this study, this aspect is not considered in the converter ratings.

4.1 Voltage rating

The rated SSOA (switching safe operating area) voltage *VSSOA* combined with the long-term stability against cosmic radiation defines the IGBT voltage rating. For improved reliability and to avoid false triggering due to cosmic radiation the maximum allowed SSOA voltage *VSSOA,max* is generally derated by approximately 40% from the maximum device voltage *Vce,max*. The margin between the maximum and the rated SSOA voltage is due to voltage spikes caused by diode reverse recovery currents. In a soft-switching environment this margin is considerably smaller. The higher voltage capability of the soft-switched IGBT can be explained by its snubbered commutation. The limited *di/dt* capability and the consequently longer turn-off time allow a higher blocking voltage capability in trade-off, at an acceptably low on-state voltage drop.

The number of series-connected IGBTs per VSC valve (*NIGBT*) depends on the DC link voltage that has to be supported. It is 112 for the soft-switched topology and 240 for the hard-switched topology. In connection with series connected semiconductor devices, it is important that a single component failure does not lead to a malfunction of the whole device. Therefore it is important that a short circuit failure mode (SCFM) is guaranteed. In this case, it is desirable to add some additional IGBTs to get a redundancy, which however is not considered in this comparison.

4.2 Current rating and losses of the proposed topology

The conduction losses depend on the on-state voltage drop across the device and the current through it. They can be calculated from the on-state threshold voltage *Vce0*, the on-state slope resistance *rce0* and the device current *Ice* as in (4). Both the on-state slope resistance and the threshold voltage depend on the device temperature.

$$Pcond = f0 \int [Vce0 \cdot Ice(t) + rce0 \cdot Ice2(t)]dt$$

The switching losses consist of turn-on and turn-off losses. Thereby, the turn-on losses are neglected, as the IGBTs turn on at zero-voltage zero-current conditions. Turn-on appears when the IGBTs take over the current from the main diodes in the opposite VSC leg, governed by successive commutations of the cycloconverter phase legs. Thus, the switching losses are assumed to consist only of turn-off losses and can be calculated from the turn-off energy *Eoff*. The turn-off energy is dependent on the turn-off current and the device temperature. Fig. 4 shows the simulated waveforms of the main transformer voltage and current at rated load. It can be seen that the IGBTs have to switch-off the maximum device current *Ice,max* during each cycle.

mf / fo

$$P_{sw} = f_0 \sum_{x=1} E_{off}(I_{ce,max}) \quad (5)$$

From the IGBT losses and the maximum device current, the required active silicon area can be calculated. As expected for a soft-switched application, the IGBT is limited by the SSOA requirement.

4.3 Current rating and losses of the reference topology

The switching losses are calculated from available switching loss data of the Cross Sound Cable project. The conduction losses are calculated according to (4). As expected for a hard-switched topology, the IGBTs are thermally limited. Thus, the current rating is determined by the conduction and switching losses. The required active silicon area is about 13 % smaller than the area required for soft-switching. Fig. 5 shows the simulated voltage and current waveform of a VSC phase leg at rated load.

The IGBT rating and losses of the back-to-back VSCs are calculated in the same way as for the main VSC. Thereby, the loss distribution between the rectifier and the inverter part within the back-to-back VSC is different. The IGBT conduction losses in the inverter are approximately five times higher than in the rectifier, whereas the switching losses are equal. This is due to the fact that the IGBTs are conducting under a major part in the inverter mode. This leads to higher IGBT losses in the inverter part of the back-to-back VSC and thus to a higher accumulated IGBT power rating (7.53 GW compared to 6.56 GW for the rectifier part). Fig. 6 shows the simulated voltage and current waveforms (including the current ripple) of an arbitrary back-to-back VSC phase leg under rated conditions.

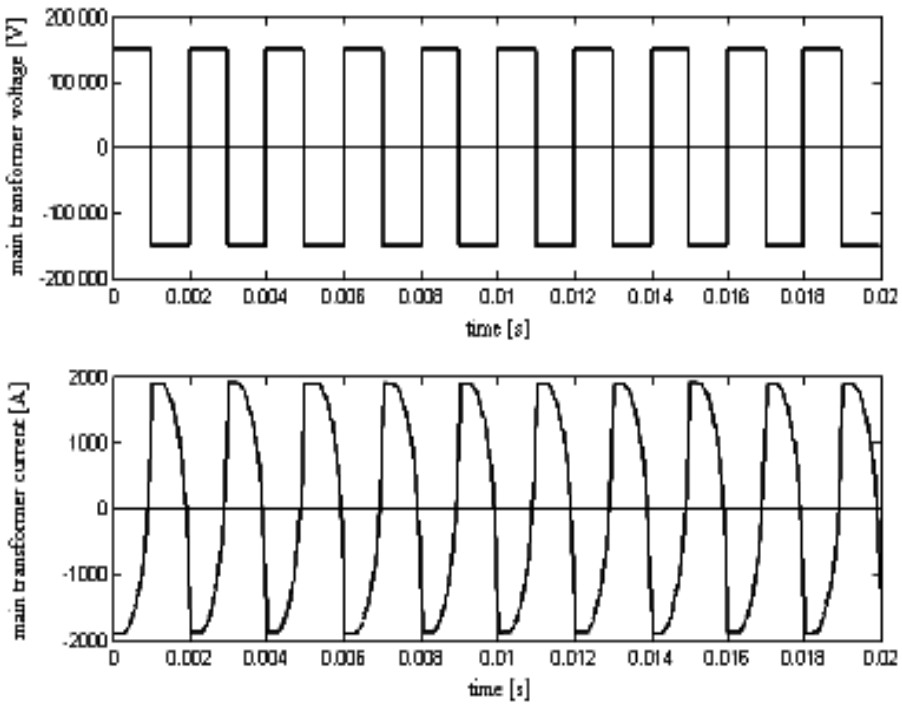

Fig. 4. Simulated waveforms of main transformer voltage and current. Operation at rated load with $m_a = 1$.

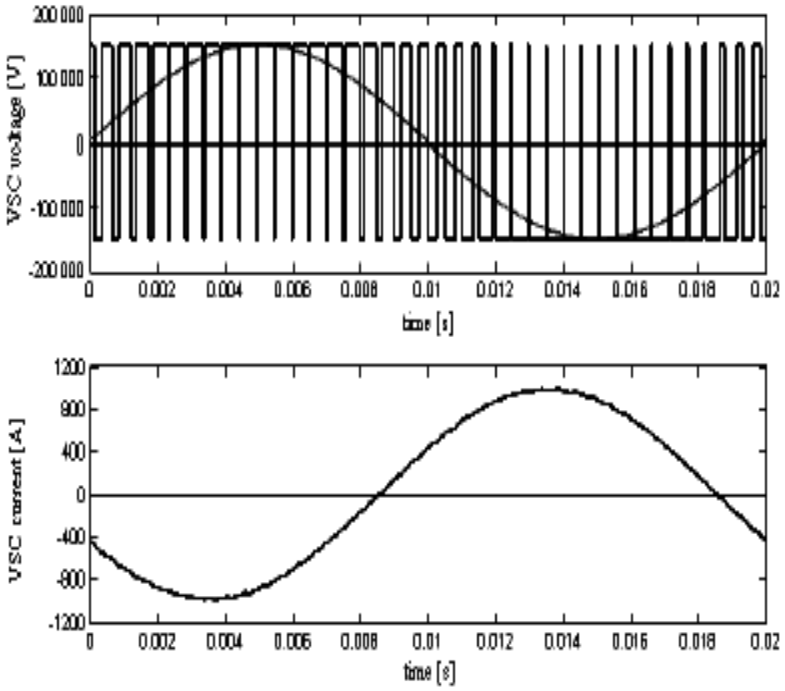

Fig. 5. Simulated voltage and current waveforms of the hard-switched VSC. Operation at rated load with $m_a = 1$.

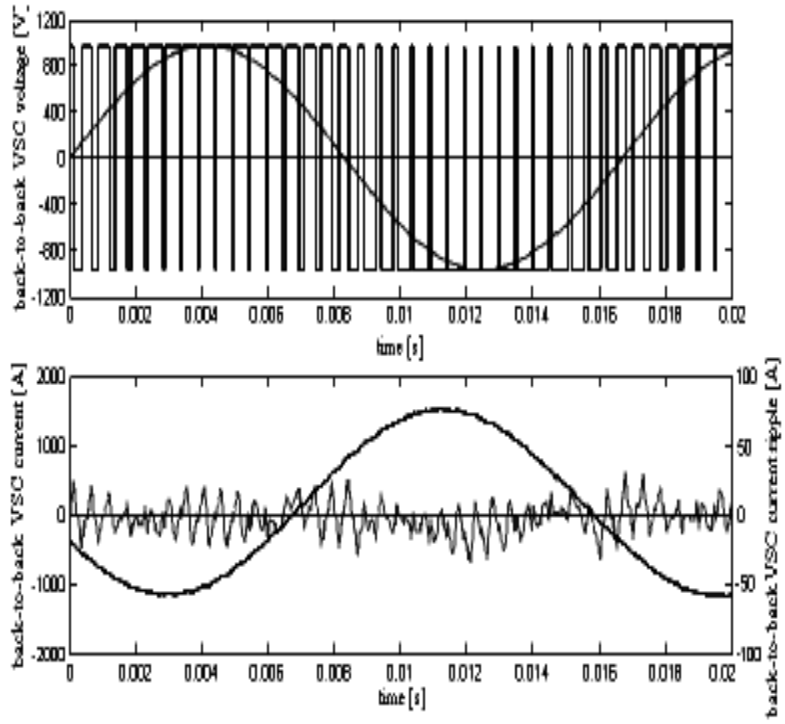

Fig. 6. Simulated voltage and current waveforms of the back-to-back VSC. Operation at rated load with $m_a = 1$.

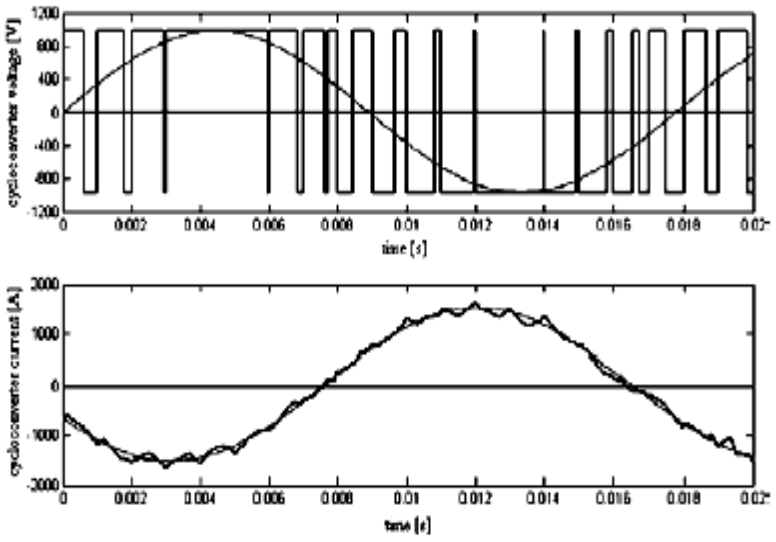

Fig. 7. Simulated waveforms of cycloconverter phase voltage and current. Operation at rated load with $m_a = 1$.

V. ADDITIONAL LOSSES

This section covers the converter losses that are not related to the IGBTs,namely diode losses in the different VSCs and thyristor losses in the cycloconverters. Additional system losses as filter, transformer or cable losses are not included in this comparative study, focusing on the converter losses and IGBT ratings.

5.1 Diode losses in the VSCs

The diode losses are an essential part of the total losses in the VSCs. In particular when the VSC operates in a rectifier mode, as it is the case in both the main VSCs. Thereby the diodes are conducting during the major part of a commutation cycle. This increases the system efficiency as the diode conduction losses are lower compared to the IGBT conduction losses. The allowed current density for the diodes is approximately twice the one for the IGBTs. This results in approximately half the silicon area for a diode compared to an IGBT.

5.2 Thyristor losses in the cycloconverters

The applied thyristors in the cycloconverters are the fast thyristors T930S from Eupec. Their electrical properties are given in Table 1.The thyristor conduction losses are calculated according to (4). Fig. 7 shows the simulated voltage and current waveform of an arbitrary cycloconverter phase leg under rated conditions. The fundamental output frequency, phase shift and current amplitude of every cycloconverter vary depending on i.e. wind conditions. The thyristor conduction losses proved to be comparably low as only one thyristor per valve is conducting at a given instant (compared to a back-to-back VSC, where always two devices are conducting). Thus, the thyristors are in average only conducting a quarter of time. The conduction losses of a cycloconverter are approximately half the ones of a back-to-back VSC.

The total thyristor losses including conduction and switching losses are calculated from a standard duty cycle supplied by the manufacturer, as given in Fig 8.

TABLE 1
THYRISTOR T930S CHARACTERISTICS

Repetitive peak forward off-state voltage V_{DRM}	1600 V
Repetitive peak reverse voltage VRRM	1800 V
RMS on-state current I_{TRMSM}	2000 A
Average on-state current I_{TAVM}	930 A
Threshold voltage VT	1.35 V
Slope resistance rT	0.33 mΩ

It shows the total thyristor losses depending on the device current *ITM* and the conduction time *tw*. The current derivative *diT/dt* during turn-on and turn-off depends on the transformer leakage inductance and cable inductances. It is designed for 50 A/µs, thus requiring 30.4 µs for a commutation of the maximum device current. This corresponds to a time period of maximum 3 % for switching a thyristor under a commutation cycle. Fig. 8 shows some simulated thyristor operation points. Thereby, an average device current was assumed in the on state during each commutation cycle. The total thyristor losses received are only a rough estimation and have to be verified experimentally later on. But as there is no detailed switching loss data available, it is the only possibility to get an indication of the real total thyristor losses.

The switching losses are calculated from the difference between the total thyristor losses and the conduction losses, and thus are only estimated as well.

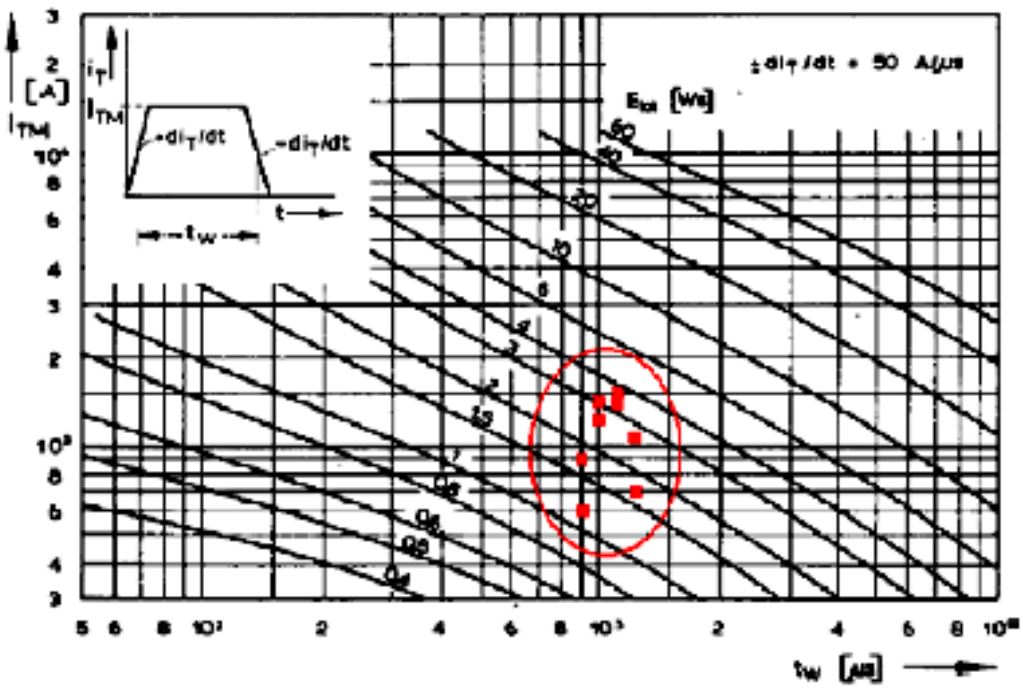

Fig. 8. Total Thyristor losses during some conduction cycles(Operation at rated load)

VI. CONCLUSION

The emergence of larger and more efficient offshore wind farms has opened new challenges in their grid connection. A number of commercial VSC transmission schemes are now in operation and show their suitability and potential. But despite the range of advantages that VSC transmission offers, the high initial costs and the switching losses limit the area of application.

The concept of a novel soft-switching AC/DC converter is presented in this paper. A single-phase VSC with capacitive snubbers connected to cycloconverters via an MF AC bus promises substantial benefits both in efficiency and initial costs. Table 2 presents an overview of the IGBT power rating and the different converter losses. It includes detailed results about the proposed soft-switched (SS) topology and the hard switched (HS) reference topology for different frequency modulation ratios *p*. A high frequency modulation ratio causes extensive switching losses but reduces the harmonic frequency distortion. The switching frequency for a frequency modulation ratio $p = 9$ is 450 Hz, which makes a comparison with the proposed topology ($mf = 500$ Hz) more significant. Table 2 also includes the power ratings and losses of the cyclo converters and the back-to-back converters (B2B) for different frequency modulation ratios *p*.

The total converter efficiency of the novel proposed topology is 99.2 % compared to an efficiency of the reference topology between 98.0 % and 94.6 depending on the frequency modulation ratio. This corresponds to a reduction of the total converter losses from 4.10 MW to 1.55 MW (for $p = 9$). Such a significant reduction is achieved by two main factors: First, the number of semiconductor devices is significantly reduced in the proposed topology. This reduces both the conduction and switching losses. Second, the application of a soft switched modulation scheme minimizes the switching losses. For instance, the main VSC switching losses are reduced by over 90 % (from 4.17 MW to 0.41 MW) for a frequency modulation ratio equal to 39. Fig. 9 shows a diagram of the switching and conduction losses of the different converters. It has to be noticed that additional losses as i.e. in the cables of the MF AC bus contribute to the total system losses in the proposed soft-switched topology.

Apart from reducing the converter losses, a reduction of the initial converter costs is highly desired. In the new proposed topology, major savings are achieved by reducing the number of semiconductor devices. Two phase legs are eliminated in the main VSC by using a single-phase VSC. A comparison with a state-of-the-art hard-switched topology shows the potential of the new topology: The IGBT power rating of the main VSC is decreased between 24 % ($p = 9$) and 70 % ($p = 39$). The IGBT power rating is calculated from the number of valves *N valve*, the number of IGBTs per valve *NIGBT*, the current rating per IGBT and the voltage rating of the IGBTs *Vce, max*. It indicates the costs that are related to the IGBTs, namely the IGBTs themselves, their gate drives and possible voltage sharing circuitries. The IGBTs in the back-to-back VSC can be replaced by comparably cheap thyristors in the cycloconverters. Another factor that contributes to reduced initial costs is the replacement of the three-phase transformers by cheaper single-phase MF transformers.

This paper showed that the proposed VSC topology offers substantial benefits in both converter efficiency and initial costs. As a consequence, the application of VSC transmission for the grid connection of wind farms gets far more attractive as the minimum cable length at which it can compete with AC transmission is decreasing.

REFERENCE

[1] Arrillaga, Jos; *"High Voltage Direct Current Transmission"*, second edition, Institution of Electrical Engineers, ISBN 0 85296 941 4, Chapter 1, pp 1-9. **1998.**

[2] Davidson, C.C., Preedy, R.M., Cao, J., Zhou, C., Fu, J., *"Ultra-High-Power Thyristor Valves for HVDC"* in Developing Countries, IET 9th International Conference on AC/DC Power Transmission, London, October **2010.**

[3] Skog, J.E., van Asten, H., Worzyk, T., Andersrød, T., Norned – *"World's longest power cable session"* Paris, paper reference B1-106. **2010.**

[4] Rowe, B.A., Goodrich, F.G., Herbert, I.R., "*Commissioning the Cross Channel H.V.D.C. link"*, GEC Review, Vol. 3, No. 2, **1987.**

[5] Praça, A., Arakari, H., Alves, S.R., Eriksson, K., Graham, J., Biledt, G., Itaipu *"HVDC Transmission System"* - 10 years operational experience, V SEPOPE, Recife, May **1996.**

[6] Peake, O., *"The History of High Voltage Direct Current Transmission"*, 3rd Australasian Engineering Heritage Conference **2009**

[7] Asplund, G.,Svensson, K., Jiang, H., Lindberg, J., Palsson, R., *"DC transmission based on voltage source converters"*, Paris, paper reference 14-302. **1998.**

[8] Lesnicar, A., Marquardt, R., *"An innovative modular multi-level converter topology for a wide power range"*, IEEE Power Tech Conference, Bologna, Italy, June **2003.**

[9] Black, R.M., *"The History of Electric Wires and Cable"*, Peter Peregrinus, London, p 95, **1983.**

[10] P. Julián, A. Oliva, P. Mandolesi, and H. Chiacchiarini, *"Output discrete feedback control of a DC-DC Buck converter,"* in Proceedings of the IEEE International Symposium on Industrial Electronics (ISIE'97), Guimaraes, Portugal, 7-11Julio pp. 925–930. **1997.**

[11] H. Chiacchiarini, P. Mandolesi, A. Oliva, and P. Julián, *"Nonlinear Analog controller for a buck converter: Theory and experimental results"*, Proceedings of the IEEE International Symposium on Industrial Electronics (ISIE'99), Bled, Slovenia, , pp. 601–606. 12–16 July **1999.**

[12] M. B. D'Amico, A. Oliva, E. E. Paolini y N. Guerin, *"Bifurcation control of a buck converter in discontinuous conduction mode"*, Proceedings of the 1st IFAC Conference on Analysis and Control of Chaotic Systems (CHAOS'06), pp. 399–404, Reims (Francia), 28 July **2006.**

[13] Oliva, A.R., H. Chiacchiarini y G. Bortolotto *"Developing of a state feedback controller for the synchronous buck converter"*, Latin American Applied Research, Volume 35, No 2, pp. 83–88. ISSN: 0327-0793. **April 2005.**

[14] Chierchie, F. Paolini, E.E. *"Discrete-time modelling and control of a synchronous buck converter"* Argentine School of Micro-Nano electronics, Technology and Applications, 2009. EAMTA 2009.1–2 pp. 5 – 10, **October 2009**.